Mirror Online Conformal Prediction with Intermittent Feedback

Bowen Wang, Matteo Zecchin, Member, IEEE, and Osvaldo Simeone, Fellow, IEEE

Abstract—Online conformal prediction enables the runtime calibration of a pre-trained artificial intelligence model using feedback on its performance. Calibration is achieved through set predictions that are updated via online rules so as to ensure long-term coverage guarantees. While recent research has demonstrated the benefits of incorporating prior knowledge into the calibration process, this has come at the cost of replacing coverage guarantees with less tangible regret guarantees based on the quantile loss. This work introduces intermittent mirror online conformal prediction (IM-OCP), a novel runtime calibration framework that integrates prior knowledge, while maintaining long-term coverage and achieving sublinear regret. IM-OCP features closed-form updates with minimal memory complexity, and is designed to operate under potentially intermittent feedback.

Index Terms—Conformal prediction, calibration, intermittent feedback, online convex optimization

I. Introduction

N safety-critical and high-stakes sequential decision-making processes, such as in robotics [1], [2], wireless communications [3], [4], finance [5], and medicine [6], [7], it is crucial to accurately quantify uncertainty in order to reliably predict the potential outcomes of given actions. Producing reliable uncertainty estimates in these scenarios is often challenging due to the non-stationarity of the data-generating distribution and to the possibility that feedback on the quality of the predictions may be only intermittently available [8].

A widely used approach to quantify uncertainty complements point predictions with prediction sets that satisfy coverage guarantees [9]. Notably, *adaptive conformal inference* (ACI) [10] converts black-box predictions into prediction sets that enjoy distribution-free, long-term coverage guarantees. This is done by adaptively adjusting prediction set sizes based on feedback about

This work was partially supported by the European Union's Horizon Europe project CENTRIC (101096379), by the Open Fellowships of the EPSRC (EP/W024101/1), and by the EPSRC project (EP/X011852/1). The authors are with the King's Communications, Learning and Information Processing (KCLIP) Lab, Department of Engineering, King's College London, London WC2R 2LS, U.K. (e-mail: {bowen.wang, matteo.1.zecchin, osvaldo.simeone}@kcl.ac.uk).

1

Methods	ACI [10]	I-ACI [16]	B-ACI [17]	IB-ACI	IM-OCP (this work)
long-term coverage	✓	√	X	X	✓
sublinear regret	\	✓	✓	√	√
prior information	X	X	√	√	√
memory complexity	√	✓	X	X	✓
closed-form update	_	✓	X	X	✓
intermittent feedback	X	✓	X	√	✓

past decisions [11]–[15]. Intermittent feedback can be accommodated via *intermittent ACI* (I-ACI) [16].

In contrast to ACI, the recently introduced *Bayesian ACI* (B-ACI) adopts a data-centric Bayesian objective that incorporates not only feedback, but also *prior information* on the prediction scores [17]. When the prior information is well specified, B-ACI can yield prediction sets with lower *regret* in terms of the quantile loss as compared to ACI. A lower regret with respect to the quantile loss implies better performance in stochastic settings with independent data [17]. However, B-ACI does not guarantee the key calibration requirement of deterministic long-term coverage. Furthermore, it requires storing past data, as well as solving a convex problem at each calibration step.

As summarized in Table I, existing online calibration schemes either cannot incorporate prior information or sacrifice long-term coverage guarantees. To address these limitations, we introduce *intermittent mirror online conformal prediction* (IM-OCP). IM-OCP builds on *online mirror descent* (OMD) [18]–[20] to integrate prior knowledge, while employing an importance weighting strategy to handle intermittent feedback [21]. This design enables IM-OCP to retain the computational and memory efficiency of ACI, while incorporating prior information. We showcase the merits of IM-OCP for the task of *received signal strength indicator* (RSSI)-based localization under intermittent feedback [22]–[24].

II. BACKGROUND

A. Online Calibration via Set Prediction

We consider the problem of online calibration in sequential decision-making problems. At each round t, a

learner observes an input $X_t \in \mathcal{X}$ and aims to predict the corresponding label $Y_t \in \mathcal{Y}$. To this end, the predictor assigns a negatively oriented $score\ s(X_t,Y)$ to each value $Y \in \mathcal{Y}$, which is assumed to be upper bounded by a constant $B < \infty$, i.e., $s(X,Y) \leq B$. For example, the quadratic loss is defined as $s(X_t,Y) = |f(X_t)-Y|^2$, where $f(X_t)$ is the prediction. Using predictor's output, a prediction set \mathcal{C}_t is produced that includes all labels $Y \in \mathcal{Y}$ with a score no larger than a threshold r_t , i.e.,

$$C_t = C(X_t, r_t) = \{ y \in \mathcal{Y} : s(X_t, Y) \le r_t \}. \tag{1}$$

After producing the decision C_t , the system receives feedback in one of the following two forms, from least to most informative: 1) miscoverage error feedback, in which the feedback signal at time t corresponds to the miscoverage error $E_t = \mathbb{1}\{Y_t \notin C_t\}$; and 2) score feedback, where the feedback corresponds to the ground truth score $r_t^* = s(X_t, Y_t)$. We assume that feedback is intermittent, so that feedback is available with probability p_t at round t.

Given a target miscoverage rate $\alpha \in [0, 1]$, the goal of calibration is to leverage the outlined feedback information to optimize, in an online fashion, the thresholds $\{r_t\}_{t=1}^T$ in (1) so as to ensure the *long-term coverage guarantee* over the time horizon T [10]

$$\operatorname{MisCov}(T) = \left| \frac{1}{T} \sum_{t=1}^{T} E_t - \alpha \right| \le A T^{-\gamma}.$$
 (2)

In (2), the parameters A and γ are constants independent of T. By (2), the rate of miscoverage errors, $\operatorname{MisCov}(T)$, on an arbitrary sequence $\{(X_t, Y_t)\}_{t=1}^T$ converges to the target miscoverage level α as the number of steps T tends to infinity.

While the condition (2) applies to an arbitrary sequence $\{(X_t,Y_t)\}_{t=1}^T$, in some settings one may be justified to assume that the sequence consists of *independent* and identically distributed (i.i.d.) samples. In this case, the probabilistic coverage condition $\Pr\{Y_t \notin \mathcal{C}_t\} = \alpha$ can be met for each time t by selecting the threshold r_t as the $(1-\alpha)$ -quantile of the score distribution. This quantile can be estimated by minimizing the empirical quantile loss

$$\ell_{1-\alpha}(r, r_t^*) = (\alpha - \mathbb{1}\{r < r_t^*\})(r - r_t^*)$$
 (3)

as $q_{\alpha}(r_{1:T}^*) = \min_{u \in \mathbb{R}} \sum_{t=1}^T \ell_{1-\alpha}(u, r_t^*)$. In fact, with i.i.d. data, the estimate $q_{\alpha}(r_{1:T}^*)$ tends to the true $(1-\alpha)$ -quantile in the limit $T \to \infty$.

To assess the capacity of a calibration procedure to perform well also in the case of i.i.d. data, it is thus useful to evaluate the extent to which the thresholds $\{r_t\}_{t=1}^T$ deviate from the estimated quantile $q_\alpha(r_{1:T}^*)$. Note that the latter can be only evaluated in hindsight, i.e., at time T, while the thresholds r_t must be produced

online at time t. This deviation is measured by the regret

$$\operatorname{Reg}(T) = \sum_{t=1}^{T} \ell_{1-\alpha}(r_t, r_t^*) - \min_{u \in \mathbb{R}} \sum_{t=1}^{T} \ell_{1-\alpha}(u, r_t^*), \quad (4)$$

which amounts to the difference between the *cumulative* quantile loss of the predicted sequence $\{r_t\}_{t=1}^T$ and the cumulative loss of the optimal fixed threshold $q_{\alpha}(r_{1:T}^*)$.

B. Adaptive Conformal Inference

Assuming that the feedback signal is always available, i.e., $p_t = 1$ for all t, ACI [10] adaptively adjusts the thresholds r_t using an *online gradient descent* (OGD) strategy based on the miscoverage error feedback E_t . Specifically, the threshold r_t is updated using the gradient of the quantile loss (3) as

$$r_{t} = r_{t-1} - \eta_{t-1} \nabla \ell_{1-\alpha}(r_{t-1}, r_{t-1}^{*})$$

= $r_{t-1} - \eta_{t-1}(\alpha - E_{t-1}),$ (5)

where $\eta_t > 0$ is the step size. Thanks to the regret guarantees of OGD and the restorative nature of the quantile loss [25], given a learning rate sequence $\eta_t = c/\sqrt{t}$ with c > 0 independent of T, ACI enjoys both sublinear regret and long-term coverage guarantee (2) with $\gamma = 1/2$ [14].

ACI has been extended to the *intermittent feedback* scenario. Denoting as obs_t the binary random variable taking value 1 if feedback E_t is observed, I-ACI [16] uses an OGD rule in which the step size is scaled as in

$$r_t = r_{t-1} - \eta_{t-1}(\alpha - E_{t-1}) \frac{\text{obs}_{t-1}}{p_{t-1}}.$$
 (6)

I-ACI is shown to satisfy expected long-term coverage and to enjoy a sublinear expected regret (see (11) and (14)) [16].

C. Bayesian Adaptive Conformal Inference

ACI and I-ACI do not allow the integration of prior knowledge about the data distribution in the calibration process. In contrast, B-ACI assumes the availability of a prior distribution P(r), with support [0, B], on the scores $\{r_t^*\}_{t\geq 1}$. Leveraging this information, along with score feedback, at each time step t, the threshold r_t is obtained by solving the convex optimization problem

$$r_t = \arg\min_{r} \left\{ \eta_t \psi(r) + \frac{1 - \eta_t}{t - 1} \sum_{i=1}^{t-1} \ell_{1-\alpha}(r, r_i^*) \right\}, \quad (7)$$

where the convex regularizing function $\psi(r) = \mathbb{E}_{r^* \sim P}[\ell_{1-\alpha}(r, r^*)]$ accounts for prior knowledge.

Unlike ACI and I-ACI, which have constant memory complexity and a simple update rule that can be computed in closed form, B-ACI requires linear memory to store the sequence $\{r_t^*\}_{t\geq 1}$ of feedback signals, and it requires to solve a convex minimization problem at

each round t. B-ACI attains sublinear regret, potentially outperforming ACI when the prior knowledge is well specified. However, B-ACI is not guaranteed to satisfy the long-term coverage condition (2).

Similar to ACI, it is possible to extend B-ACI to handle *intermittent feedback*. This variant, referred to here as IB-ACI, obtains the threshold r_t by minimizing the sum of the importance-weighted losses

$$r_t = \arg\min_{r} \left\{ \eta_t \psi(r) + \frac{1 - \eta_t}{t - 1} \sum_{i=1}^{t-1} \ell_{1-\alpha}(r, r_i^*) \frac{\text{obs}_i}{p_i} \right\}.$$
(8)

In Appendix A, we show that IB-ACI achieves sub-linear expected regret (see (14)).

III. INTERMITTENT MIRROR ONLINE CONFORMAL PREDICTION

Given the state of the art summarized in Table I, this paper introduces IM-OCP, a novel prior-dependent calibration scheme with intermittent feedback that exhibits low complexity, sublinear regret, and coverage guarantees. IM-OCP tackles the problem of online calibration via an OMD strategy [18]–[20]. This way, IM-OCP retains the simplicity and performance guarantees of first-order methods such as ACI, while allowing for the incorporation of prior information.

For a given prior distribution P(r) defined in [0, B] for the scores r^* and a parameter $\sigma > 0$, IM-OCP introduce a regularizing function $R(\cdot)$ of the form

$$R(r) = \mathbb{E}_{r^* \sim P}[\ell_{1-\alpha}(r, r^*)] + \frac{\sigma}{2}|r|^2, \tag{9}$$

where the first term follows B-ACI, while the second term ensures the strong convexity of the function $R(\cdot)$. In Appendix B, we show that the regularizing function (9) is closed, differentiable, μ -strongly convex for some real number $\mu > \sigma$, and L-smooth for some real number $L \leq \max_{r \in [0,B]} \{P(r)\} + \sigma$.

Given the regularizing function R(r), the associated Bregman divergence is denoted as $\mathcal{B}_R(u,v) = R(u) - R(v) - (\nabla R(v))^T (u-v)$. The corresponding *mirror map* is given by $\mathcal{M}(\cdot) = \nabla R(\cdot)$, with its inverse map defined as $\mathcal{M}^{-1}(\cdot) = (\nabla R)^{-1}(\cdot)$.

At each time t, IM-OCP updates the threshold via the OMD rule

$$r_{t} = \mathcal{M}^{-1} \left(\mathcal{M}(r_{t-1}) - \eta_{t-1} (\alpha - E_{t-1}) \frac{\text{obs}_{t-1}}{p_{t-1}} \right).$$
(10)

When the feedback E_{t-1} is not observed, and thus we have $obs_{t-1} = 0$, the update (10) corresponds to the identity map. In contract, when the feedback E_{t-1} is observed, the update (10) amounts to a gradient descent step in the dual space associated with the mirror map.

A. Theoretical Guarantees

We now analyze the performance of IM-OCP, showing that it satisfies expected long-term coverage while also enjoying sublinear expected regret. Proofs are deferred to Appendix C.

In the following, IM-OCP coverage is measured via its expected miscoverage error

$$\overline{\text{MisCov}}(T) = \left| \mathbb{E} \left[\frac{1}{T} \sum_{t=1}^{T} E_t \right] - \alpha \right|, \quad (11)$$

which corresponds to the absolute difference between the expected fraction of miscoverage errors, where the expectation is taken over the feedback observations $\{obs_t\}_{t=1}^T$, and the target coverage level α .

Similarly to [14], we first establish the following ancillary result stating that the iterates produced by IM-OCP are bounded.

Lemma 1. For any $r_1 \in [0, B]$, the iterates produced by IM-OCP satisfy the condition

$$r_{t} \in \left[-\frac{\alpha \varpi_{t}}{\mu}, B + \frac{(1-\alpha)\varpi_{t}}{\mu} \right] \text{ for } t > 1, \qquad (12)$$

$$\text{where } \varpi_{t} = \max_{i \in [1, \dots, t-1]} \{ \eta_{i} / p_{i} \}.$$

Equipped with Lemma 1, we characterize the expected miscoverage error rate of IM-OCP as follows.

Theorem 1. For any non-increasing step size sequence $\{\eta_t\}_{t\geq 1}$, the miscoverage error rate of IM-OCP satisfies the inequality

$$\overline{\text{MisCov}}(T) \le \frac{1}{T\eta_T} \left(LB + \frac{L\eta_1}{\mu p_{\min}} \right), \quad (13)$$

where $p_{\min} = \min_{t \in [1, 2, \dots, T]} \{p_t\}.$

We now prove that IM-OCP enjoys sublinear regret. Similar to (11), we define the IM-OCP regret as

$$\overline{\operatorname{Reg}}(T) = \mathbb{E}\left[\sum_{i=1}^{T} \ell_{\alpha}(r_{i}, r_{i}^{*}) \frac{\operatorname{obs}_{i}}{p_{i}}\right] - \min_{u \in \mathbb{R}} \sum_{i=1}^{T} \ell_{\alpha}(u, r_{i}^{*}),$$
(14)

Like (4), the quantity in (14) measures the difference between the expected cumulative quantile loss of IM-OCP and the loss of the best threshold chosen in hindsight having observed the entire sequence $\{r_t^*\}_{t>1}$.

Theorem 2. For any non-increasing step size sequence $\{\eta_t\}_{t\geq 1}$, the regret of IM-OCP in (14) satisfies the inequality

$$\overline{\text{Reg}}(T) \le \frac{D_T}{\eta_T} + \frac{1}{2\mu p_{\min}} \sum_{i=1}^T \eta_i, \tag{15}$$

where
$$D_T = \max_{t \in \{1,...,T\}} \mathcal{B}_R(q_{\alpha}(r_{1:T}^*), r_t).$$

Theorems 1 and 2 provide bounds on the expected miscoverage error rate and regret of IM-OCP as a

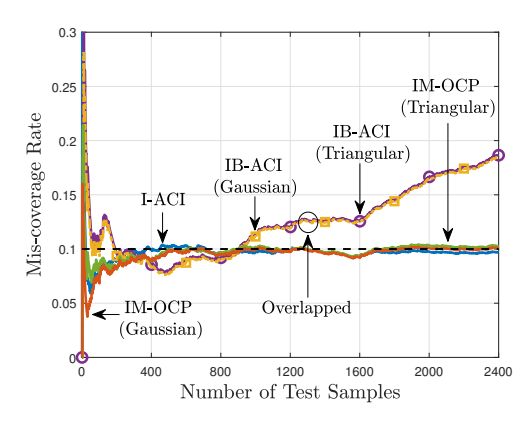


Fig. 1. Miscoverage rate versus the number of test samples ($\alpha = 0.1$).

function of the learning rate sequence. The following corollary specializes the miscoverage and regret guarantee under a judicious choice of the learning rate.

Corollary 1. With a fixed learning rate $\eta = cT^{-\beta}$ or a decaying learning rate $\eta_t = ct^{-\beta}$, where c is a positive constant independent of T, IM-OCP satisfies the miscoverage guarantee (2) with $\gamma = 1 - \beta$ and has regret $\text{Reg}(T) = \mathcal{O}(T^{\max\{\beta, 1-\beta\}})$.

IV. NUMERICAL RESULTS

In this section, we present numerical results for an RSSI-based localization problem assuming intermittent feedback.

A. Setting

We consider a multi-building, multi-floor indoor localization problem and adopt the UJIIndoorLoc dataset [26]. The goal is to localize a device positioned in one of three buildings based on the signal power received from M = 520 access points [22]–[24]. Accordingly, the input $X_t \in \mathbb{R}^M$ corresponds to an M-dimensional vector of RSSI values, while the label $Y_t = [Y_t^{\text{Log}}, Y_t^{\text{Lat}}]^T \in$ \mathbb{R}^2 represents the longitude and latitude coordinates of the corresponding device to be localized. We apply online calibration to a pre-trained localization model $\hat{Y}_i = f_{\text{ELM}}(X_i)$, implemented using an extreme learning machine with a hidden layer of size 256 [24]. The model is trained using a training set consisting of 1000, 2000, and 8000 samples randomly selected from Buildings 1, 2, and 3, respectively. Since the accuracy of $f_{\rm ELM}(\cdot)$ is expected to increase in the building index i, due to the increasingly larger datasets as i grows, we set a decreasing probability of receiving feedback as $p_1 = 0.5$ for the first building, $p_2 = 0.3$ for the second, and $p_3 = 0.1$ for the third.

B. Results

We perform online calibration of the base predictor using I-ACI, B-ACI, and IM-OCP, considering both

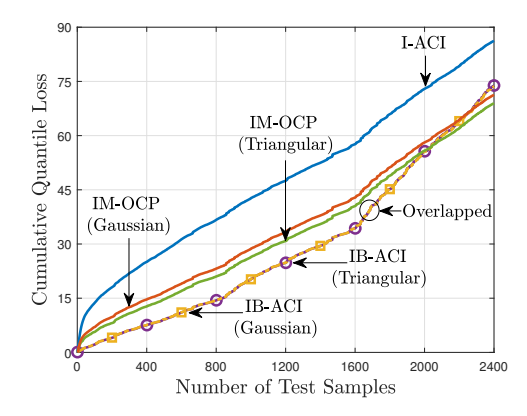


Fig. 2. Cumulative quantile loss versus the number of test samples ($\alpha = 0.1$).

triangular and truncated Gaussian prior distributions P(r) defined in the interval [0,B]. Specifically, for the triangular prior distribution, the mode is set to 0.1, while for the truncated Gaussian prior distribution, the mean is set to 0.1 and the variance to 2. For all schemes, we consider a held-out data sequence of length T=2400, with samples randomly selected from each building with equal probability, and set the target miscoverage rate to $\alpha=0.1$.

In Fig. 1, we present the miscoverage rate as a function of time index t. Both IM-OCP and ACI, which satisfy the miscoverage guarantee (2), exhibit a miscoverage rate that converges to the target value α . In contrast, IB-ACI, which does not come with a theoretical coverage guarantee, obtains a final miscoverage rate higher than the target value.

In Fig. 2, we report the cumulative quantile loss for all algorithms. By leveraging prior information, IM-OCP achieves a lower cumulative loss—and consequently, a smaller regret—compared to I-ACI, while remaining competitive with B-ACI.

Overall, these results demonstrate that IM-OCP satisfies the coverage guarantees while incorporating prior information and achieving a lower regret compared to I-ACI.

V. CONCLUSION

We have proposed IM-OCP, an OCP scheme for intermittent feedback scenarios based on OMD, which uses importance sampling to handle intermittent feedback. IM-OCP allows the incorporation of prior knowledge about the calibration task via the specification of a mirror map, and is proven to achieve both sublinear regret and miscoverage guarantees. The practical effectiveness of IM-OCP is demonstrated through its application to an RSSI-based localization problem. Future work may extend this study to multi-agent online calibration and explore online calibration under robustness requirements to impairments such as missing data.

REFERENCES

- D. Kulić and E. A. Croft, "Safe planning for human-robot interaction," *Journal of Robotic Systems*, vol. 22, no. 7, pp. 383–396, 2005.
- [2] L. Lindemann, M. Cleaveland, G. Shim, and G. J. Pappas, "Safe planning in dynamic environments using conformal prediction," *IEEE Robotics and Automation Letters*, 2023.
- [3] K. M. Cohen, S. Park, O. Simeone, P. Popovski, and S. Shamai, "Guaranteed dynamic scheduling of ultra-reliable low-latency traffic via conformal prediction," *IEEE Signal Processing Let*ters, vol. 30, pp. 473–477, 2023.
- [4] M. Zecchin, S. Park, and O. Simeone, "Forking uncertainties: Reliable prediction and model predictive control with sequence models via conformal risk control," *IEEE Journal on Selected Areas in Information Theory*, 2024.
- [5] E. Lockwood, "Predicting the unpredictable: Value-at-risk, performativity, and the politics of financial uncertainty," *Review of international political economy*, vol. 22, no. 4, pp. 719–756, 2015.
- [6] J. Vazquez and J. C. Facelli, "Conformal prediction in clinical medical sciences," *Journal of Healthcare Informatics Research*, vol. 6, no. 3, pp. 241–252, 2022.
- [7] C. Lu, A. Lemay, K. Chang, K. Höbel, and J. Kalpathy-Cramer, "Fair conformal predictors for applications in medical imaging," in *Proceedings of the AAAI Conference on Artificial Intelligence*, vol. 36, no. 11, 2022, pp. 12008–12016.
- [8] Y. Mao, C. You, J. Zhang, K. Huang, and K. B. Letaief, "A survey on mobile edge computing: The communication perspective," *IEEE communications surveys & tutorials*, vol. 19, no. 4, pp. 2322–2358, 2017.
- [9] V. Vovk, A. Gammerman, and G. Shafer, *Algorithmic learning* in a random world. Springer, 2005, vol. 29.
- [10] I. Gibbs and E. Candes, "Adaptive conformal inference under distribution shift," Advances in Neural Information Processing Systems, vol. 34, pp. 1660–1672, 2021.
- [11] S. Feldman, L. Ringel, S. Bates, and Y. Romano, "Achieving risk control in online learning settings," *Transactions on Machine Learning Research*, 2023.
- [12] A. Bhatnagar, H. Wang, C. Xiong, and Y. Bai, "Improved online conformal prediction via strongly adaptive online learning," in *International Conference on Machine Learning*. PMLR, 2023, pp. 2337–2363.
- [13] A. Angelopoulos, E. Candes, and R. J. Tibshirani, "Conformal pid control for time series prediction," *Advances in neural* information processing systems, vol. 36, pp. 23 047–23 074, 2023.
- [14] A. N. Angelopoulos, R. F. Barber, and S. Bates, "Online conformal prediction with decaying step sizes," arXiv preprint arXiv:2402.01139, 2024.
- [15] M. Zecchin and O. Simeone, "Localized adaptive risk control," in *The Thirty-eighth Annual Conference on Neural Information Processing Systems*, 2024.
- [16] M. Zhao, R. Simmons, H. Admoni, A. Ramdas, and A. Bajcsy, "Conformalized interactive imitation learning: Handling expert shift and intermittent feedback," arXiv preprint arXiv:2410.08852, 2024.
- [17] Z. Zhang, Z. Lu, and H. Yang, "The benefit of being bayesian in online conformal prediction," arXiv preprint arXiv:2410.02561, 2024
- [18] F. Orabona, "A modern introduction to online learning," *arXiv* preprint arXiv:1912.13213, 2019.
- [19] S. Shalev-Shwartz et al., "Online learning and online convex optimization," Foundations and Trends® in Machine Learning, vol. 4, no. 2, pp. 107–194, 2012.

- [20] E. Hazan *et al.*, "Introduction to online convex optimization," *Foundations and Trends*® *in Optimization*, vol. 2, no. 3-4, pp. 157–325, 2016.
- [21] V. Elvira and L. Martino, "Advances in importance sampling," arXiv preprint arXiv:2102.05407, 2021.
- [22] K. Wu, J. Xiao, Y. Yi, D. Chen, X. Luo, and L. M. Ni, "Csi-based indoor localization," *IEEE Transactions on Parallel and Distributed Systems*, vol. 24, no. 7, pp. 1300–1309, 2012.
- [23] H. Si, X. Guo, N. Ansari, C. Chen, L. Duan, and J. Huang, "Environment-aware positioning by leveraging unlabeled crowdsourcing data," *IEEE Internet of Things Journal*, vol. 11, no. 9, pp. 16436–16449, 2024.
- [24] H. Sifaou and O. Simeone, "Semi-supervised learning via cross-prediction-powered inference for wireless systems," *IEEE Transactions on Machine Learning in Communications and Networking*, vol. 3, pp. 30–44, 2025.
- [25] A. N. Angelopoulos, M. I. Jordan, and R. J. Tibshirani, "Gradient equilibrium in online learning: Theory and applications," arXiv preprint arXiv:2501.08330, 2025.
- [26] J. Torres-Sospedra, R. Montoliu, A. Martínez-Usó, J. P. Avariento, T. J. Arnau, M. Benedito-Bordonau, and J. Huerta, "UJIIndoorLoc: A new multi-building and multi-floor database for WLAN fingerprint-based indoor localization problems," in 2014 international conference on indoor positioning and indoor navigation (IPIN). IEEE, 2014, pp. 261–270.

1

Mirror Online Conformal Prediction with Intermittent Feedback

Bowen Wang, Matteo Zecchin, Member, IEEE, and Osvaldo Simeone, Fellow, IEEE

(Supplementary Material)

APPENDIX A REGRET BOUND OF IB-ACI

We now show that IB-ACI with a decreasing step size $\eta_t=t^{-1/2}/2$ enjoys a sublinear expected regret.

We define $h_t = \frac{\eta_t(t-1)}{1-\eta_t}$ and express IB-ACI update rule as follows

$$r_t = \arg\min_{r} h_t \psi(r) + \sum_{i=1}^{t-1} \ell_{1-\alpha}(r, r_i^*) \frac{\text{obs}_i}{p_i}.$$
 (A-1)

Based on [19, Lemma 2.3], we have

$$\sum_{i=1}^{T} \ell_{1-\alpha}(r_i, r_i^*) \frac{\text{obs}_i}{p_i} - \sum_{i=1}^{T} \ell_{1-\alpha}(u, r_i^*) \frac{\text{obs}_i}{p_i} \\
\leq h_T \psi(u) + \sum_{i=1}^{T} \left(\ell_{1-\alpha}(r_i, r_i^*) - \ell_{1-\alpha}(r_{i+1}, r_i^*)\right) \frac{\text{obs}_i}{p_i}.$$
(A-2)

Noticing that $\ell_{1-\alpha}(r,r_i^*)\frac{\mathrm{obs}_i}{p_i}$ is $\frac{\mathrm{obs}_i}{p_i}$ -Lipschitz, and with the additional assumption that $\psi(r)$ is ϵ -Lipschitz, it follows that $h_t\psi(u)$ is $h_t\epsilon$ -Lipschitz and that

$$\ell_{1-\alpha}(r_i, r_i^*) \frac{\operatorname{obs}_i}{p_i} - \ell_{1-\alpha}(r_{i+1}, r_i^*) \frac{\operatorname{obs}_i}{p_i}$$

$$\leq \frac{\operatorname{obs}_i}{p_i} |r_i - r_{i+1}| \leq \frac{\operatorname{obs}_i}{p_i^2 h_i \epsilon}$$
(A-3)

By combining (A-2) and (A-3), we obtain

$$\sum_{i=1}^{T} \ell_{1-\alpha}(r_i, r_i^*) \frac{\text{obs}_i}{p_i} - \sum_{i=1}^{T} \ell_{1-\alpha}(u, r_i^*) \frac{\text{obs}_i}{p_i}$$

$$\leq h_T \psi(u) + \sum_{i=1}^{T} \frac{\text{obs}_i}{p_i^2 h_i \epsilon}$$
(A-4)

Taking expectation over the sequence $\{obs_i\}_{i=1}^T$

$$\operatorname{Reg}(T) \leq \mathbb{E}_{\operatorname{obs}_{i} \sim p_{i}} \left[h_{t} \psi(u) + \sum_{i=1}^{T} \frac{\operatorname{obs}_{i}}{p_{i}^{2} h_{i} \epsilon} \right]$$

$$\leq h_{T} \psi(u) + \sum_{i=1}^{T} \frac{1}{p_{i} h_{i} \epsilon}$$

$$\leq h_{T} \psi(u) + \sum_{i=1}^{T} \frac{1}{p_{\min} h_{i} \epsilon},$$
(A-5)

where $p_{\min} = \min\{p_i\}$. For the step size choice $\eta =$

 $1/(2\sqrt{t})$, we have $h_t = \mathcal{O}(\sqrt{t})$ and $1/h_t = \mathcal{O}(1/\sqrt{t})$. Thus, IB-ACI achieves sub-linear regret

$$\operatorname{Reg}(T) \leq \mathcal{O}\left(\psi(u)\sqrt{T} + \sum_{i=1}^{T} \frac{1}{p_{\min}\epsilon\sqrt{t}})\right) \sim \mathcal{O}(\sqrt{T}). \tag{A-6}$$

APPENDIX B

PROOF OF STRONGLY CONVEX AND SMOOTHNESS

The prior regularizer can be expressed as

$$\begin{split} R(r) = & \mathbb{E}_{r_i^* \sim P}[\ell_{1-\alpha}(r, r_i^*)] + \frac{\sigma}{2} |r|^2 & \text{(B-1a)} \\ = & \int_0^B \ell_{1-\alpha}(r, r^*) P(r^*) \mathrm{d}r^* + \frac{\sigma}{2} |r|^2 & \text{(B-1b)} \\ = & (\alpha - 1) \int_r^B (r - r^*) P(r^*) \mathrm{d}r^* \\ & + \alpha \int_r^a (r - r^*) P(r^*) \mathrm{d}r^* + \frac{\sigma}{2} |r|^2. & \text{(B-1c)} \end{split}$$

where P(r) is the probability density functions of prior distribution P in domain [0, B].

The first derivative of R(r) is

$$\nabla R(r) = \alpha \int_0^r P(r^*) dr^* + (\alpha - 1) \int_r^B P(r^*) dr^* + \sigma r$$

$$= \alpha - \int_r^B P(r^*) dr^* + \sigma r$$

$$= \int_0^r P(r^*) dr^* - (1 - \alpha) + \sigma r$$

$$\stackrel{(a)}{=} \begin{cases} \text{CDF}_P(r) - (1 - \alpha) + \sigma r, & 0 \le r \le B \\ -(1 - \alpha) + \sigma r, & r < 0 \\ \alpha + \sigma r, & r > B \end{cases}$$
(B-2)

where $\mathrm{CDF}_P(r) = \int_0^r P(r^*) \mathrm{d}r^*$ denotes the cumulative distribution function (CDF) of the prior distribution $P(r^*)$, and (a) follows from the prior distribution $P(r^*)$ being defined over [0,B], while $P(r^*)=0$ for $r^* \notin [0,B]$, $\mathrm{CDF}_P(r^*)=1$ for r>B, and $\mathrm{CDF}_P(r^*)=0$ for r<0.

While, the second derivative of R(r) is given by

$$\nabla^2 R(r) = \begin{cases} P(r) + \sigma, & 0 \le r \le B \\ \sigma, & \text{otherwise} \end{cases}$$
 (B-3)

Since $\sigma > 0$, we have that $\nabla^2 R(r) = P(r) + \sigma > \sigma$ for all $r \in [0, B]$. It follows that R(r) is μ -strongly convex with $\mu \geq \sigma$. Similarly, $\nabla^2 R(r) = P(r) + \sigma \leq \max_r \{P(r)\} + \sigma$, which implies that R(r) is L-smoothness with $L \leq \max_r \{P(r)\} + \sigma$.

APPENDIX C

PROOF OF THEORETICAL GUARANTEES IN SEC. III-A

In this appendix, we provide a detailed derivation of the theoretical guarantees presented in Sec. III-A. We begin by deriving the bound on the iterates, then establish the miscoverage guarantee and regret bound, and finally discuss the impact of the learning rate on the miscoverage guarantee and regret.

A. Proof of Lemma 1

Recalling the definition of the mirror map $\mathcal{M}(\cdot) = \nabla R(\cdot)$, the update in the dual space of IM-OCP corresponds to

$$\nabla R(r_t) - \nabla R(r_{t-1}) = -\eta_{t-1}(\alpha - E_{t-1}) \frac{\text{obs}_{t-1}}{p_{t-1}}.$$
(C-1)

Having assumed the mirror map to be μ -strongly convex, it holds

$$\langle \nabla R(r_t) - \nabla R(r_{t-1}), r_t - r_{t-1} \rangle$$

$$\geq \mu \|r_t - r_{t-1}\|^2$$
(C-2)

and

$$\langle \nabla R(r_t) - \nabla R(r_{t-1}), r_t - r_{t-1} \rangle$$

$$\leq \frac{1}{\mu} \left\| \nabla R(r_t) - \nabla R(r_{t-1}) \right\|^2.$$
(C-3)

Leveraging these two inequalities, we now show by contradiction that the value of the threshold r_t is upper bounded by $B+(1-\alpha)\varpi_t$ μ for all t. Recall that $\varpi_t=\max_{i=1,\dots,t-1}\eta_i/p_i$ and hence the sequence $\{\varpi_t\}_{t\geq 1}$ is non-decreasing. Assume, without loss of generality, that t is the first instant in which the iterate $r_t>B+(1-\alpha)\varpi_t$ μ . Given that ϖ_t is non-decreasing in t, it follows that $r_t>r_{t-1}$. From inequality (C-2) it follows

$$r_t \le r_{t-1} - \frac{\eta_{t-1}}{\mu} (\alpha - E_{t-1}) \frac{\text{obs}_{t-1}}{p_{t-1}},$$
 (C-4)

from which we conclude that $E_{t-1} = 1$ and $\operatorname{obs}_{t-1} = 1$ in order for the inequality $r_t > r_{t-1}$ be true. At the same time, given that $E_{t-1} = 1$ and $\operatorname{obs}_{t-1} = 1$, inequality (C-3) implies that

$$r_{t-1} \ge r_t + \frac{\eta_{t-1}(\alpha - 1)}{\mu p_{t-1}} > B,$$
 (C-5)

where the last inequality follows from having initially assumed that $r_t > B + (1 - \alpha)\varpi_t \mu$. However, this

last inequality leads to a contradiction. In fact, since for $r_{t-1} > B$, we have must have $E_{t-1} = 0$ and $\operatorname{obs}_{t-1} = 1$. The lower bound follows similarly.

B. Proof of Theorem 1

Note that for IM-OCP it holds that $\mathbb{E}[\nabla R(r_{t+1})]$

$$= \mathbb{E}[\nabla R(r_{\tau})] - \mathbb{E}\left[\sum_{t=\tau}^{T} \eta_{t}(E_{t} - \alpha) \frac{\text{obs}_{t}}{p_{t}}\right]$$

$$= \mathbb{E}[\nabla R(r_{\tau})] - \sum_{t=\tau}^{T} \eta_{t}(\mathbb{E}[E_{t}] - \alpha).$$
(C-6)

Define $\Delta_1 = 1/\eta_1$ and $\Delta_i = 1/\eta_i - 1/\eta_{i-1}$, and note that $1/\eta_t = \sum_{i=1}^t \Delta_i$. The expected miscoverage rate at time T is given by

 $\overline{\text{MisCov}}(T)$

$$= \left| \mathbb{E} \left[\frac{1}{T} \sum_{i=1}^{T} \left(\sum_{\tau=1}^{i} \Delta_{\tau} \right) \eta_{i}(E_{i} - \alpha) \right] \right|$$

$$= \left| \mathbb{E} \left[\frac{1}{T} \sum_{\tau=1}^{T} \Delta_{\tau} \left(\sum_{i=\tau}^{T} \eta_{i}(E_{i} - \alpha) \right) \right] \right|$$

$$\leq \frac{1}{T} \sum_{\tau=1}^{T} |\Delta_{\tau}| \cdot \left| \mathbb{E} \left[\sum_{i=\tau}^{T} \eta_{i}(E_{i} - \alpha) \right] \right|$$

$$\leq \frac{\|\Delta_{1:T}\|_{1}}{T} \cdot \max_{\tau \in \{1, \dots, T\}} \left| \sum_{i=\tau}^{T} \eta_{i}(\mathbb{E} \left[E_{i} \right] - \alpha) \right|.$$
(C-7)

From (C-6), it holds that

$$\sum_{i=\tau}^{T} \eta_i(\mathbb{E}\left[E_i\right] - \alpha) = \mathbb{E}\left[\nabla R(r_{T+1}) - \nabla R(r_{\tau})\right], \quad \text{(C-8)}$$

which allows us to rewrite (C-7) as

 $\overline{\mathrm{MisCov}}(T)$

$$\leq \frac{\|\Delta_{1:T}\|_{1}}{T} \max_{\tau \in \{1,\dots,T\}} \left| \mathbb{E} \left[\nabla R(r_{T+1}) - \nabla R(r_{\tau}) \right] \right|. \tag{C-9}$$

Since R(r) is an L-smooth function, we obtain

$$\max_{\tau \in \{1, \dots, T\}} |\mathbb{E} \left[\nabla R(r_{T+1}) - \nabla R(r_{\tau}) \right]| \\
\leq \max_{\tau \in \{1, 2, \dots, T\}} L |\mathbb{E} \left[r_{T+1} - r_{\tau} \right]| \\
\leq LB + \frac{L\eta_{1}}{\mu p_{\min}}, \tag{C-10}$$

where the last inequality follows from Lemma 1 and from the assumption of a non-increasing step size sequence $\{\eta_t\}_{t\geq 1}$.

By plugging (C-10) into (C-9) and noting that $\|\Delta_{1:T}\|_1 = 1/\eta_T$, we achieve the final result

$$\overline{\text{MisCov}}(T) \le \frac{1}{T\eta_T} \left(LB + \frac{L\eta_1}{\mu p_{\min}} \right).$$
 (C-11)

C. Proof of Theorem 2

For any sequence $\{obs_t\}_{t\geq 1}$ and $u\in \mathbb{R}$, online mirror descent satisfies [18, Theorem 6.10]

$$\sum_{t=1}^{T} \ell_{1-\alpha}(r_t, r_t^*) \frac{\text{obs}_t}{p_t} - \sum_{t=1}^{T} \ell_{1-\alpha}(u, r_t^*) \frac{\text{obs}_t}{p_t} \\
\leq \frac{D_T}{\eta_T} + \frac{1}{2\mu} \sum_{t=1}^{T} \eta_t \left| \nabla \ell_{1-\alpha}(r_t, r_t^*) \frac{\text{obs}_t}{p_t} \right|^2,$$
(C-12)

where $D_T = \max_{t \in [1,T]} \mathcal{B}_R(u, r_t)$. Taking expectations over the random variables $\{\text{obs}_t\}_{t \geq 1}$ and noting that

$$\mathbb{E}\left[\left|\nabla \ell_{1-\alpha}(r_i, r_i^*) \frac{\mathsf{obs}_i}{p_i}\right|\right] \le \mathbb{E}\left[\left|\frac{\mathsf{obs}_i}{p_i}\right|\right] = 1, \quad \text{(C-13)}$$

it follows that

Reg(T)

$$= \mathbb{E}\left[\sum_{i=1}^{T} \ell_{\alpha}(r_{i}, r_{i}^{*}) \frac{\text{obs}_{i}}{p_{i}}\right] - \sum_{i=1}^{T} \ell_{\alpha}(u, r_{i}^{*})$$

$$\leq \frac{D_{T}}{\eta_{T}} + \frac{1}{2\mu} \sum_{i=1}^{T} \frac{\eta_{i}}{p_{i}} \leq \frac{D_{T}}{\eta_{T}} + \frac{1}{2\mu p_{\min}} \sum_{i=1}^{T} \eta_{i},$$
(C-14)

where $p_{\min} = \min\{p_i\}$. Setting $u = q_{\alpha}(r_{1:T}^*)$ we obtain the final result.

D. Proof of Corollary 1

For fixed learning rate, by submitting $\eta=cT^{-\beta}$ into miscoverage error rate and regret bound, we have

$$\begin{split} \overline{\mathrm{MisCov}}(T) \leq & \frac{LB}{c} T^{\beta-1} + \frac{L}{c\mu p_{\mathrm{min}}} T^{-1} \\ & \sim \mathcal{O}(AT^{\beta-1}), \end{split} \tag{C-15}$$

and

$$\overline{\text{Reg}}(T) \le \frac{D_T}{c} T^{\beta} + \frac{c}{2\mu p_{\min}} T^{1-\beta}
\sim \mathcal{O}(T^{\beta} + T^{\beta-1}) = \mathcal{O}(T^{\max\{\beta,\beta-1\}}).$$
(C-16)

Similarly, for decaying learning rate, by submitting $\eta=ct^{-\beta}$ into miscoverage error rate and regret bound, we have

$$\overline{\text{MisCov}}(T) \le \frac{LB\mu p_{\min} + Lc}{\mu p_{\min} c} T^{\beta - 1} \sim \mathcal{O}(AT^{\beta - 1}).$$
(C-17)

and

$$\overline{\text{Reg}}(T) = \frac{D_T T^{\beta}}{c} + \frac{c}{2\mu p_{\min}} \sum_{t=1}^{T} t^{-\beta}
\sim \mathcal{O}(T^{\beta} + T^{1-\beta}) = \mathcal{O}(T^{\max\{\beta,\beta-1\}}).$$
(C-18)

By setting $\beta=1/2$, i.e., $\eta_t=c\sqrt{t}$, IM-OCP achieves sub-linear regret while ensuring the coverage guarantee.